Fatigue in Continuous Fibre Reinforced Thermoplastic Composites

Alberto Pertuz, Sergio Díaz-Cardona, Octavio Andrés González Estrada

Fatigue in Continuous Fibre Reinforced Thermoplastic Composites

Alberto D. Pertuz[2*], Sergio Díaz-Cardona[1], Octavio A. González-Estrada[1]

[1] GIEMA, School of Mechanical Engineering, Universidad Industrial de Santander, Carrera 27 calle 9, Bucaramanga, Colombia.

[2] GIC, School of Mechanical Engineering, Universidad Industrial de Santander, Carrera 27 calle 9, Bucaramanga, Colombia.

[*] E-mail: apertuzc@uis.edu.co

Abstract

Additive manufacturing (AM) technologies have been applied with success in many applications, being fused deposition modelling (FDM) the most widely used AM technique for fabricating thermoplastic pieces. The thermoplastic parts made by FDM present lack of strength and low stiffness, as required for fully functional and load-bearing parts. Due to this restriction, a new technology to reinforce with fibres the thermoplastic filaments was developed in the last years. Continuous fibre reinforced thermoplastic composites (CFRTPC) printers are taking this technology to a whole new level in terms of efficient production and mechanical properties. Static mechanical properties, as well as fatigue behaviour, were studied since in these types of loads a wide range of engineering dynamic applications can be envisaged. Tensile tests were performed to characterise the static mechanical properties. Fatigue tests were done to analyse the durability behaviour of the FDM composite materials, and the fracture surface was analysed by SEM microscopy. The results showed that carbon fibre isotropic layers had the higher ultimate tensile stress, with 165 MPa. From fatigue tests, stress vs. number of cycles curves (S vs N_f) in the temporary life zone were obtained. It is observed from the results that specimens with nylon matrix, triangular filling pattern and matrix density of 20%, reinforced with carbon fibre at 0-degrees, showed better

fatigue performance, increasing significantly the number of cycles before rupture of the specimen. The parameters for the Basquin's equation were found ($S = A \cdot N_f^b$), with A=206 MPa, and b= -0,039. Accordingly, mechanical characterization of continuous fibre reinforced thermoplastic composites was investigated, showing the potential use as a composite material for engineering applications.

Keywords

Continuous fibre reinforced thermoplastic composites (CFRTPC), fused deposition modelling (FDM), additive manufacturing (AM), fatigue in thermoplastics.

Introduction

Additive Manufacturing – Fused Deposition Modeling.

Additive manufacturing (AM) is a process of joining materials, layer upon layer, in order to create objects from 3D model data [1]. With AM technologies, it is possible to manufacture prototypes or functional pieces with geometries which are difficult to be produced by conventional fabrication methods [2], [3]. In comparison with conventional methods, AM is more effective since it can reduce the design-manufacturing cycle and, thus, decrease the production cost and increase the competitiveness [4],[5]. Among the AM techniques, fused deposition modelling (FDM) is the most widely used method, because of its low cost and the minimal material wasted [6]. Currently, the majority of the feedstock used in FDM are thermoplastic filaments, such as, polycarbonate (PC), polylactide (PLA), polyamide (PA), etc. [7].

Thermoplastic matrix reinforced with continuous fibres.

Nowadays, thermoplastic-matrix fibre-reinforced composites are widely used in aerospace, medical, and automobile industry and electronics applications [8], [9]. However, the thermoplastic parts made by FDM suffer from the lack of strength needed

for fully functional and load-bearing parts used in engineering applications [10]. Due to this condition, new technologies to reinforce with continuous fibres the thermoplastic filaments have recently emerged to improve the mechanical properties of the produced parts [7], [10]. Therefore, FDM offers the possibility of manufacturing complex functional and structural parts with continuous fibre reinforced thermoplastic composites (CFRTPC).

CFRTPC printers are taking this technology to a whole new level in terms of efficient production and mechanical properties [5]. Melenka et al. [11] evaluated the elastic properties of the CFRTPC printed on the MarkOne printer, and predicted the elastic properties using a volume average stiffness (VAS) method. The specimens were printed varying the volume fraction of the fibres. The results showed that an increase in the volume fraction of fibre reinforcement results in an increase in stiffness and ultimate strength of the specimen. Ning et al. [7] tested the effect of adding carbon fibre with different content and length to improve the mechanical properties of different parts fabricated by FDM. Effects on the tensile properties, i.e., tensile strength, Young's modulus, toughness, yield strength and ductility, were experimentally investigated, finding an increase in the tensile strength and in Young's modulus, but a decrease in the toughness and ductility of the specimens tested. Yang et al. [12] studied the mechanism of 3D printers for CFRTPC. They performed several mechanical tests such as three-point bending, tensile and interlaminar shear in order to characterize the CFRTPC mechanical properties. The results showed an improvement of the 10 wt% CCF/ABS specimens in the flexural and tensile strength with 127 MPa and 147 MPa, respectively, which is greater than the ABS specimens and close to the CCF/ABS (injection moulding) with the same fibre content.

Van der Klift et al. [5] evaluated the capabilities of the Mark One 3D printer in CFRTPC with carbon fibres. They printed several CFRTPC specimens with three different configurations and made a tensile test in the longitudinal direction to evaluate the mechanical properties of the specimen. The results showed an improvement in the tensile properties. Also, they found that the behaviour of the CFRTPC is not in complete agreement with the traditional mixing rules for composites due to the delamination and the formation of cavities. The results showed that the discontinuities of the fibres produced a premature failure in the areas where the fibres were absent. Tian et al. [13] introduced a mechanism for FDM of CFRTPC to produce pieces for aerospace applications and analysed the influence of the process parameters, such as, the content of the fibre and its orientation, on the mechanical properties of CFRTPC specimens. Nanya Li et al. [14] performed a study with CFRTPC polylactic acid (PLA) printed by the rapid prototyping approach. The PLA suffered a modification with a methylene chloride agent to increment the interfacial strength between carbon fibre and resin. The results of the mechanical tests showed an increment of the tensile and flexural strength of 13,8% and 164%, respectively, for the modified carbon fibre reinforced composites compared to original carbon fibre reinforced specimens. Also, they found an increment of the storage modulus of about 166% and 351% for the modified carbon fibre reinforced composites compared to PLA and original fibre reinforced specimens.

Fatigue in fused deposition modelling

In the last years, the fatigue behaviour of plastics has called attention due to their applications in aerospace, automotive and biomedical industries [15]. Afrose et al. [16] examined the fatigue behaviour of (PLA) parts processed by FDM. They performed fatigue tests in agreement with ASTM D638, for different build orientations and

percentage nominal values of the ultimate tensile stress. Specimens manufactured in X-direction showed the longest lifetime for stresses greater than 15 MPa. Around 10e4 load cycles, an important reduction in the stress could be seen in all directions. The S-N curves for the X and Y directions converged after 3000 load cycles and after 10e5 load cycles, almost coincided. No direction could be recognized after around 10e6 load cycles. The results for the tension-tension fatigue tests demonstrated that +45/-45° specimens had the longest fatigue life for each stress level, followed by the 0°, 45° and 90° orientations. Furthermore, the results showed anisotropic behaviour on the raster orientations, a different number of cycles to failure for the raster orientations and similar failure modes as those seen in static tests.

Ziemian et al. [17] performed a tensile-fatigue test on layered acrylonitrile butadiene styrene (ABS) components fabricated by FDM, following the ASTM D638 standard. This test was performed for different raster orientations and ultimate tensile stresses. The results showed dependence to various parameters such as stress amplitude, manufacturing defects present in the specimens, temperature, frequency and environment. The specimens manufactured with raster orientation at +45/-45° presented higher fatigue life and a higher storage modulus, followed by the 0, 45 and 90º orientations for the same applied loads.

Fatigue in fibre reinforced thermoplastics

Many factors, such as processing conditions, fibre length and orientation, properties and configuration of the composite matrix, interfacial properties and testing conditions, have an important effect in the fatigue behaviour of discontinuous fibre reinforced polymer matrix composites [18], [19]. Goel et al. [20] studied the fatigue behaviour of long fibre reinforced thermoplastic composites (polypropylene/20 volume % E-glass fibre) in terms of stress – number of cycles to failure curves. After testing specimens along the

longitudinal and transversal direction, they established that the specimens tried along longitudinal direction performed better under the same fatigue loading conditions. The fatigue life diminished with the increment in frequency. They associated this response with the hysteretic heating that takes place at high frequencies and, furthermore, because of the poor thermal conductivity properties of the thermoplastic matrix. Because long fibre reinforced thermoplastics have higher thermal conductivity than not reinforced thermoplastics and, subsequently, quicker heat dissipation to the surroundings occur, they demonstrated a lower temperature rise contrasted with the not reinforced cases.

To predict the fatigue life in fibre reinforced thermoplastics is a difficult task [18]. They are anisotropic and show a variety of damage mechanisms. There are a considerable number of empirical formulas in the literature to predict fatigue of composites [21], however, they are constrained to particular loading restrictions and environment. The fatigue damage process has both creep and fatigue effect. Creep tends to relax the strains and increase the fatigue life of the composite part [22]. The importance of the creep strain accumulation during the fatigue is very important. The accumulated creep strain relaxes local stresses and, subsequently, substantially modifies the predicted fatigue life. Regardless of this well-known phenomenon, coupling of physics-based methodologies for durability prediction of fibre reinforced thermoplastics combining fatigue with creep have been implemented. Fertig et al. [23] proposed a physics-based fatigue methodology based on the kinetic theory of fracture (KTF), which has been successfully implemented to predict fatigue and creep of composite structures. KTF models the damage mechanism as a thermally activated process and uses the physics of the matrix material to keep track of the damage accumulated in the composite. The steps of the process are: (i) link volume-averaged composite stresses and strains to volume-

averaged matrix stresses and strains, (ii) evaluate the damage in the matrix due to fatigue using KTF, (iii) analyse and compare the microscopic bond breaking and the macroscopic behaviour of the structure [22]. Several fatigue models have been used to predict the fatigue life of composite materials. Basquin's model [24] is used because of its simplicity and that it can be related to the fibre reinforced composite using:

$$S = A \cdot N_f^{\,b} \quad [1]$$

where S is the tensile stress, N_f is the cycles to failure, A and b are material constants, which are related to the ultimate static stress and the dynamic hardening modulus, respectively.

In this paper, the fatigue behaviour of continuous fibre reinforced thermoplastic composites made of a nylon matrix with fibreglass, Kevlar, or carbon fibres is investigated. The specimens are produced by fused deposition modelling in agreement with the ASTM D638 standard. Fatigue tests were conducted following the ASTM D7791 for composite parts under tensile fatigue loading conditions to obtain the S-N curves. Effects of the filling percentage, filling pattern of the nylon matrix, fibre materials, and fibre orientation, as well as, the number of concentric rings used in the printing configuration were investigated.

Materials and methods

The specimens were printed in the Mark Two© FDM printer from MarkForged Inc [25]. The printing parameters used for manufacturing both tensile and fatigue tests specimens are specified in Table 1. Specimens with a total of 32 layers and a nylon matrix with triangular and hexagonal filling patterns for the honeycomb core were used, considering filling densities of 20% and 50%.

The two types of reinforcement used in the nylon matrix are:

- Isotropic layers of fibreglass, Kevlar and carbon fibre as reinforcement material at orientations of 0, 45, and 60 degrees.
- Concentric rings of continuous fibres of fibreglass, Kevlar and carbon fibre.

The specimen geometry was imported from a stereolithographic file (STL) to the printer software Eiger©. The software allows changing several printing parameters such as filling percentage, filling pattern and number of nylon or fibre reinforcement layers, as shown in Table 1.

Uniaxial tensile tests were carried out according to ASTM D638-14 (Standard Test Method for Tensile Properties of Plastics) using the dimensions of the type IV specimen. A total of three samples per condition were tested. Such tests were performed using an MTS-Bionix universal testing machine model 370.02, with a load cell of 25 KN, at an advance speed of 5 mm/min, grip distance of 28 millimetres and the longitudinal strain and transversal section contraction were determined using the LVDT and the laser extensometer LX500, respectively.

The characterization of fatigue properties under uniaxial tensile loading is performed according to ASTM D7791-14 (Standard Test Method for Uniaxial Fatigue Properties of Plastics) procedure A, for rigid and semi-rigid plastics, with a stress relation of R=0.1 in tensile-tensile condition. The life/stress curve vs. the number of cycles (S vs N_f) was estimated under the condition of temporary life of composite materials. The standard establishes testing specimens with a maximum stress corresponding to different percentages of the ultimate tensile stress (S_{UT}) obtained in uniaxial tensile tests, i.e., 95, 90, 85 y 80 % S_{UT}. Twenty (20) test specimens for condition were tested (5 test specimens per percentage point), at a testing frequency of 5 Hz. Once the results were obtained, the Weibull's statistical method was implemented to adjust the median per

points tested. Finally, the four levels of stress of the S vs N_f curve were obtained for the composite material.

A fractographic evaluation was performed to analyse the micromechanical structure of the composite, as well as the failure mechanisms under tensile and fatigue loading conditions. A JEOL, JSM 6490-LV scanning electron microscope was used to perform the fractographic analysis. Samples were covered with a gold nanolayer, allowing proper observation of the fractured zones.

Results and analysis

Uniaxial tensile test

The uniaxial tensile tests performed show the ultimate tensile stress (S_{UT}) and the strain of the specimens. The optimal printing parameters are determined based on the S_{UT}. Figure 1 shows the uniaxial tensile test results for nylon matrices printed with filling patterns and densities of triangular 20%, triangular 50%, and hexagonal 50%. The curves represent the average of three tests performed. The results show that triangular filling pattern have the higher ultimate tensile stress value, with 17 MPa. Also, triangular configurations increase the stiffness of the specimens.

Figure 2 shows the results for isotropic fibreglass layers printed at different fibre angle orientations w.r.t. the longitudinal direction, i.e., 0°, 45° and 60°. The filling is set to triangular pattern at 20%. As expected, the results show that the optimal fibre angle orientation in the isotropic layers is at 0 degrees, with an ultimate tensile stress value of 124 MPa.

Figure 3 presents the results for different fibre materials used in the isotropic layers at 0-degree orientation: Kevlar, carbon and fibreglass. The results show that carbon fibre isotropic layers have the higher ultimate tensile stress value, with 165 MPa.

In Figure 4, a comparison between two different reinforcement configurations using concentric rings is shown. Concentric rings reinforcement in carbon fibre are printed in two different configurations: (i) two rings and four layers, and (ii) four rings and two layers. The results show that the two rings and four layers configuration presents the higher ultimate tensile stress value was 114 MPa.

Given these static results, with ultimate tensile stresses up to 165 MPa, we can notice the potential of additive manufacturing of continuous fibre reinforced thermoplastic composites for producing functional parts for engineering applications. However, due to the various printing parameters and material configurations, there is a gap to be filled in terms of design considerations, and more information should be provided to be able to guarantee the final result.

Fatigue under uniaxial tension-tension test

Basquin´s model is used to represent the fatigue test results. The model relates logarithmically the stress (S) of the composite with the number of cycles to failure (N_f), for loading conditions of 95, 90, 85, and 80% of the ultimate tensile stress (S_{UT}), as indicated by the ASTM D3479/D3479M−12 standard. The Weibull distribution is selected as the statistical method for the adjustment of the data obtained at each load level. By adjusting the data with this statistical tool, we can obtain a precise mean for the number of cycles of the material at each respective load level.

The goodness test for the data fit analysis in each of the Weibull analyses is done under the Kolmogorov-Smirnov test, with confidence intervals of 90 to 95 per cent. Thus, with a P-Value higher than 0.05 - 0,1 we cannot reject the hypothesis that the data adjust to a Weibull distribution, i.e., the data fit the Weibull model with a 90-95 percent reliability.

Using the Statgraphics® software, the Weibull analysis is performed, and curves are constructed for each respective filling percentage and filling pattern of the matrix.

Effects of the filling percentage and the filling pattern of the matrix

The filling percentage and filling pattern of the nylon matrix are varied, as shown in Table 2. The experiment has been structured to discard the less favourable results. The data obtained from the experiments related to the specimens for each of the filling patterns and filling percentage is shown in Table 3. Figure 5 shows the test results (stress fatigue (S) vs number of cycles to failure (N_f)) carried out to 95, 90, 85, 80% of the ultimate tensile stress (S_{UT}) and amplitude of continuous stress for nylon matrix with triangular filling pattern and 20% of filling percentage. If compared with the literature review, it shows the typical life expectancy of continuous fibre reinforced thermoplastic composite materials. Fractures occur at relatively low life cycles, which can be attributed to the first fibre that fractures quickly, as it is seen in static tensile behaviour. Conversely, it can be observed that the studied composite material shows a small cycle dispersion due to the presence of cyclical charges close to its ultimate tensile stress (S_{UT}). However, this dispersion increases as the applied load decreases. This is revealed by the fact that the standard deviation in the rupture cycles in the first point is 22.2 cycles, while it is 206.6 cycles for the triangular filling pattern and 20% filling percentage.

Figure 6 shows the results of S vs N_f curves for filling patterns of triangular 20%, 50%, and hexagonal 50%. It is observed from Figure 6 that the nylon matrix with a filling percentage of 20% and triangular filling pattern presents the optimum performance S-N_f curve since, comparatively, under the characteristic loads of the experiment, it presents a relatively greater number of life cycles before the rupture of the material, which translates into a curve of semi-bell shape wider than the others.

The specimens printed without fibre reinforcement show elastoplastic behaviour. Most of these specimens have a yield failure, their strain overcome the test machine displacement. Only a few specimens filled with triangular pattern at 50% show a fracture failure. Table 4 collects the Basquin's parameters found by Weibull fitting at 95, 90, 85, 80% of S_{UT} of the curves shown in Figure 6. Notice that the triangular 50% has the highest values for parameters *A* and *b*, showing that it is the most resistant and ductile material. It is important to note that the specimens are of plastic origin. On the other hand, parameters for triangular 20% and hexagonal 50% are very similar. It is an equivalent adjustment value for the linear regression R^2 for all conditions studied. Henceforth, we continue the study with triangular 20%, since it consumes less material in specimen manufacture and the properties are similar.

Effects of the fibre orientation

We study the effect of fibre orientation in the fatigue life, considering a nylon matrix with fibreglass as reinforcement material. Optimum angle is evaluated and, then, different reinforcement materials are tested, and it is analysed which of them presents the best performance in the *S* vs N_f curve. This second phase of the study is developed under the same methodology shown in the preceding section for obtaining the optimal filling percentage and filling patterns.

Table 5 shows the variables of the experiment in this second stage, we set to triangular filling pattern and 20% filling percentage, reinforced with fibreglass at 0, 45, and 60 degrees. Table 6 collects the results of the fatigue tests. It can be observed that for high values of Weibull mean probability stresses the dispersion is smaller than for lower values of Weibull mean probability stresses. Also, all values at 95% S_{UT} are below 150 cycles, showing that the fibreglass yields a great fragility to the composite.

Figure 7 shows the results of S vs N_f curves fitted to the Basquin´s model, for a nylon matrix with triangular filling pattern, 20% of filling percentage, reinforced with fibreglass at 0, 45, and 60 degrees. From Figure 7, the nylon reinforced with fibreglass at 0 degrees shows better performance, increasing the number of cycles before rupture of the specimen.

As the angle varied from zero degrees, the material begins to fail due to yield and not rupture. In addition to this, the nylon matrix elongates in a similar way as it did in the tests without any reinforcing fibre.

The failures observed in the specimens reinforced with fibreglass at 60 degrees (and some specimens with fibreglass at 45 degrees), at load percentages of 85% and 80% of the ultimate tensile stress, are similar to the failures in the specimens without fibre reinforcement. Notice that the greater the inclination of the fibre, more percentage of the load is absorbed by the nylon matrix, causing the nylon matrix deformation.

Table 7 shows the results of the values A and b of Basquin's parameters for the nylon matrix with the triangular filling pattern, 20% of filling percentage, reinforced with fibreglass to 0, 45, 60 degrees. Notice that the nylon reinforced with fibreglass to 0 degrees has the higher value for parameter A, although the parameter b is low, showing that the reinforcement with fibreglass at 0 degrees increases the final resistance of the composite, and also produces a high fragility. Regarding the equivalent adjustment value for the linear regression R^2, fibreglass at 0° presents the best adjustment for the three conditions studied. The two other orientations at 45 and 60 degrees have very low fatigue resistance, prevailing the condition of fibre orientation above the reinforcement stress.

Effects of the fibre reinforcement material

In this section different materials to reinforce the nylon matrix are tested, and it is analysed which of them presents the best performance in the S vs N_f curves of fatigue properties. Table 8 shows the variables of the experiment, considering a triangular filling pattern and 20% filling percentage, reinforced with fibreglass, carbon, and Kevlar fibre at 0 degrees. Table 9 displays the results of the fatigue tests. Note that for high values of Weibull mean probability stresses, the dispersion is smaller than for lower values of Weibull mean probability stresses. Also, all values at four load levels % of S_{UT} reinforced with carbon fibre show a very high number of cycles to rupture, compared to the other fibres, indicating that the carbon fibre under the conditions studied shows the best fatigue properties.

Figure 8 shows the results of S vs N_f curves fitted to the Basquin´s model, nylon matrix with the triangular filling pattern, 20% of filling percentage, reinforced with fibreglass, Kevlar and carbon fibre at 0 degrees orientation. Notice that the nylon matrix reinforced with carbon fibre showed better performance, increasing significantly the number of cycles before rupture of the specimens. Specimens having reinforcement with Kevlar and fibreglass showed a comparable relative behaviour, although the intersections of stress axis are different and the tendencies to fatigue life axis also vary.

A considerable number of specimens reinforced with carbon fibre (isotropic layers at 0 degrees and concentric rings) break in the change of the transversal area section. It was observed that in most of the specimens, the fibre reinforcement in this zone was absent, especially in the specimens reinforced with concentric rings.

Table 10 shows the results of the values A and b of Basquin's parameters for the nylon matrix with the triangular filling pattern, 20% of filling percentage, reinforced with fibreglass, Kevlar and carbon fibre at 0 degrees orientation. Notice that specimens with carbon fibre have the highest values for parameter A, although the parameter b is low,

showing that the reinforcement with carbon yields a fragile composite. They also have a tendency to stabilise at high number of cycles in the fatigue life axis, which indicates good properties for fatigue applications. The parameter *b* for carbon and Kevlar fibres are similar, remarking a similar fragility, but the carbon fibre is more resistant, and its equivalent adjustment value for the linear regression R^2 represents an acceptable fit.

Finally, based on the S-N curves shown in Figure 8, for a specimen with a nylon matrix, triangular filling pattern, 20% of filling percentage, the best performance is achieved when the material is reinforced with carbon fibres at a zero degrees orientation, increasing the number of cycles for each of the characteristic loads of the experiment. The specimens with carbon fibre reinforcement that showed a higher number of cycles had fibre reinforcement in the change of the transversal area section.

Effects of the concentric ring reinforcement

In this section, we investigate the response for different configurations of the concentric ring reinforcement, for the nylon matrix with previously established characteristics.

Table 11 includes the variables of the experiment, for a triangular filling pattern and 20% filling percentage, reinforced with carbon fibre, considering: 2 ring-type, 4 layers, and 4 ring-type, 2 layers reinforcements. Table 12 shows the results of the fatigue tests, high dispersion can be observed in failure cycles for both conditions, for example, at 90% S_{UT}, 2 rings 4 layers, the lowest is 4 cycles and the highest is 72050 cycles. This dispersion can be attributed to premature fracture of reinforced fibres, the fractured fibres lead to a localized stress concentration with consequent accelerated fracture.

Figure 9 shows the results of S vs N_f curves fitted to the Basquin´s model, nylon matrix with the triangular filling pattern, 20% of filling percentage, reinforced with carbon-fibre, 2 ring-type, 4 layers “A”, “B”, and 4 ring-type, 2 layers reinforcement. It is observed that the specimens with 2 ring-type, 4 layers “A” showed a better

performance, increasing significantly the number of cycles before rupture, but its equivalent adjustment value for the linear regression R^2 present an unacceptable fit (0.5), which is attributed to the value at 90% S_{UT}. This value was extracted, and the curve was adjusted (Carbon fibre, 2 ring-type, 4 layers "B"). This procedure presented an equivalent adjustment value for the linear regression R^2 with an acceptable fit.

Although the reinforcement with 4 ring-type, 2 layers showed an acceptable behaviour, the intersections of stress axis are different and the tendencies to fatigue life axis are comparable.

Table 13 shows the results of the values *A* and *b* of Basquin's parameters for the nylon matrix with the triangular filling pattern, 20% of filling percentage, reinforced with carbon fibre, 2 ring-type, 4 layers, and 4 ring-type, 2 layers. Notice that 2 Rings, 4 layers has the highest value for the parameter *A*, although the parameter *b* is low, showing that the reinforcement yields a fragile composite with a tendency of the fatigue life axis to stabilise at high number of cycles. Premature fibre failures was presented. The parameter *b* for 2 Rings, 4 Layers, "B" and 4 Rings, 2 Layers are similar, remarking a similar fragility.

Finally, based on the *S* vs N_f curves shown in Figure 9, for a specimen with: nylon matrix with the triangular filling pattern, 20% of filling percentage, the best performance is achieved when the material is reinforced with carbon fibre and 2 Rings, 4 layers, thus, increasing the number of cycles for each of the characteristic loads of the experiment.

Fractographic analysis

Figure 10 and Figure 11 show the fracture zone for the carbon fibre reinforced specimens with triangular filling pattern, 20% of filling percentage, and 0° fibre orientation, at 80 and 95% of S_{UT}, respectively. Figure 12 and Figure 13 show the

fracture zone for the specimen with Kevlar fibre at 80 and 95% of S_{UT}. Notice the fusion of the nylon layers across the cross section and the reinforcement fibres in the upper layers. In Figure 10 and Figure 12, the fracture in the upper part of the nylon matrix show incipient beach lines that can be attributed to the fatigue tests. Comparatively, it is observed that the beach lines are present in the nylon matrix but not in the reinforcing fibres, since they show a different damage mechanism.

With respect to the reinforcement with carbon fibres, it can be observed that the fracture of the fibres was more uniform in the specimens tested at 80% of S_{UT}, as shown in Figure 10. In the specimens tested at 95% of S_{UT}, it is observed in Figure 11 that some fibres were longer than others due to the loading conditions.

Comparatively, it can be observed that in the specimens reinforced with Kevlar fibre, the fibres are more continuous, since Kevlar is a more ductile material than carbon fibre. In Figure 13, the fracture of the specimens reinforced with Kevlar fibre shows the formation of knots in the fibres, while in the specimens reinforced with carbon fibre, the fibres break straight, as shown in Figure 10.

Conclusions

It was observed that the optimal filling pattern for the nylon matrix without reinforcement was triangular, with a filling percentage of 20%. Comparatively, this configuration bears approximately 150 more load cycles N in the 95% S_{UT} and 500 more load cycles N in the 80% S_{UT}. The specimens printed without fibre reinforcement showed an elastoplastic behaviour. Most of these specimens had a yield failure, and their elastoplastic strain exceeded the test machine displacement.

The results showed that the optimal fibre angle orientation was at 0 degrees. Compared with the 45 degrees and 60 degrees configurations, it bore approx. 100 MPa more in

each one of the S_{UT} percentages. The number of the load cycles N was almost the same for all the configurations.

The break failures observed in the specimens reinforced with fibreglass at 60 degrees (and some specimens with fibreglass orientated at 45 degrees), at load percentages of 85% and 80% of S_{UT}, were similar to the failures in the specimens without fibre reinforcement.

The results concluded that the nylon matrix reinforced with carbon fibre layers oriented at 0° degrees presents better fatigue response. The number of load cycles N was higher in each of the S_{UT} percentages, as shown in Figure 9. A considerable number of specimens reinforced with carbon fibre (isotropic layers at 0 degrees and concentric rings) broke in the change of the transversal area section. The specimens with carbon fibre reinforcement that showed a greater of number cycles had fibre reinforcement in the change of the transversal area section.

The reinforcement configuration with concentric rings of 2 rings, 4 layers, showed a better fatigue response that the 4 rings, 2 layers configuration. Approximately 40 MPa or more was tolerated in each one of the S_{UT} percentages. For the 90 % and 95% of S_{UT}, the 2 rings, 4 layers configuration present more load cycles N, as shown in Table 20 and Table 21.

The effect of the humidity in the specimens was observed. A specimen per each load percentage in all the experiments was left at atmospheric humidity conditions. The results showed that the specimens without fibre reinforcement were more susceptible to the effect of the humidity than the specimens with fibre reinforcement. These specimens showed yield failures at lower load cycles than the specimens conserved at the humidity-controlled condition. Further work includes studies regarding different variables, such as the effect of combined loads.

Acknowledgements

The authors acknowledge the support of project FM-2018-1, Convocatoria VIE, Universidad Industrial de Santander, and the Electron Microscopy Laboratory at Universidad Industrial de Santander, PTG, Guatiguará, for their cooperation in the fractographic analysis.

References

[1] "Standard terminology for additive manufacturing technologies," *ASTM F2792-12a*. West Conshohocken, PA, 2012.

[2] M. Alimardani, E. Toyserkani, and J. P. Huissoon, "Three-dimensional numerical approach for geometrical prediction of multilayer laser solid freeform fabrication process," *J. Laser Appl.*, vol. 19, no. 1, pp. 14–25, 2007.

[3] A. Yakovlev, E. Trunova, D. Grevey, M. Pilloz, and I. Smurov, "Laser-assisted direct manufacturing of functionally graded 3D objects," *Surf. Coatings Technol.*, vol. 190, no. 1, pp. 15–24, 2005.

[4] R. Hague, I. Campbell, and P. Dickens, "Implications on design of rapid manufacturing," *J. Mech. Eng. Sci.*, vol. 217, no. 1, pp. 25–30, 2003.

[5] F. Van Der Klift, Y. Koga, A. Todoroki, M. Ueda, Y. Hirano, and R. Matsuzaki, "3D Printing of Continuous Carbon Fibre Reinforced Thermo-Plastic (CFRTP) Tensile Test Specimens," *Open J. Compos. Mater.*, vol. 06, no. 01, pp. 18–27, 2016.

[6] P. Dudek, "FDM 3D printing technology in manufacturing composite elements," *Arch. Metall. Mater.*, vol. 58, no. 4, pp. 1415–1418, 2013.

[7] F. Ning, W. Cong, J. Qiu, J. Wei, and S. Wang, "Additive manufacturing of

carbon fiber reinforced thermoplastic composites using fused deposition modeling," *Compos. Part B Eng.*, vol. 80, pp. 369–378, 2015.

[8] S. Ahn, M. Montero, D. Odell, S. Roundy, and P. K. Wright, "Anisotropic material properties of fused deposition modeling ABS," *Rapid Prototyp. J.*, vol. 8, no. 4, pp. 248–257, 2002.

[9] S. J. Leigh, R. J. Bradley, C. P. Purssell, D. R. Billson, and D. A. Hutchins, "A Simple, Low-Cost Conductive Composite Material for 3D Printing of Electronic Sensors," *PLoS One*, vol. 7, no. 11, p. e49365, Nov. 2012.

[10] W. Zhong, F. Li, Z. Zhang, L. Song, and Z. Li, "Short fiber reinforced composites for fused deposition modeling," *Mater. Sci. Eng. A301*, vol. 301, pp. 125–130, 2001.

[11] G. W. Melenka, B. K. O. Cheung, J. S. Schofield, M. R. Dawson, and J. P. Carey, "Evaluation and prediction of the tensile properties of continuous fiber-reinforced 3D printed structures," *Compos. Struct.*, vol. 153, pp. 866–875, 2016.

[12] C. Yang, X. Tian, T. Liu, Y. Cao, and D. Li, "3D printing for continuous fiber reinforced thermoplastic composites: mechanism and performance," *Rapid Prototyp. J.*, vol. 23, no. 1, pp. 209–215, 2017.

[13] X. Tian, Z. Hou, D. Li, and B. Lu, "3D printing of continuous fiber reinforced composites with a robotic system for potential space applications," 2016.

[14] N. Li, Y. Li, and S. Liu, "Rapid prototyping of continuous carbon fiber reinforced polylactic acid composites by 3D printing," *J. Mater. Process. Technol.*, vol. 238, pp. 218–225, 2016.

[15] N. S. F. Jap, G. M. Pearce, A. K. Hellier, N. Russell, W. C. Parr, and W. R. Walsh, "The effect of raster orientation on the static and fatigue properties of filament deposited ABS polymer," *Int. J. Fatigue*, vol. 124, pp. 328–337, Jul.

2019.

[16] M. F. Afrose, S. H. Masood, P. Iovenitti, M. Nikzad, and I. Sbarski, “Effects of part build orientations on fatigue behaviour of FDM-processed PLA material,” *Prog. Addit. Manuf.*, vol. 1, no. 1–2, pp. 21–28, 2016.

[17] S. Ziemian, M. Okwara, and C. W. Ziemian, “Tensile and fatigue behavior of layered acrylonitrile butadiene styrene,” *Rapid Prototyp. J.*, vol. 21, no. 3, pp. 270–278, 2015.

[18] A. Krairi, I. Doghri, and G. Robert, “Multiscale high cycle fatigue models for neat and short fiber reinforced thermoplastic polymers,” *Int. J. Fatigue*, vol. 92, pp. 179–192, Nov. 2016.

[19] M. Eftekhari and A. Fatemi, “Variable amplitude fatigue behavior of neat and short glass fiber reinforced thermoplastics,” *Int. J. Fatigue*, vol. 98, pp. 176–186, May 2017.

[20] A. Goel, K. K. Chawla, U. K. Vaidya, N. Chawla, and M. Koopman, “Characterization of fatigue behavior of long fiber reinforced thermoplastic (LFT) composites,” *Mater. Charact.*, vol. 60, no. 6, pp. 537–544, 2009.

[21] J. Brunbauer and G. Pinter, “Stiffness and strength based models for the fatigue-life prediction of continously fiber reinforced composites,” *Mater. Sci. Forum*, vol. 825, pp. 960–967, 2015.

[22] F. H. Bhuiyan and R. S. Fertig, “A Physics-Based Combined Creep and Fatigue Methodology,” no. January, pp. 1–8, 2017.

[23] K. Kuhn and R. S. Fertig III, “A Physics-Based Fatigue Life Prediction for Composite Delamination Subject to Mode I Loading,” *Am. Soc. Compos. Thirty-First Tech. Conf.*, 2016.

[24] O. H. Basquin, “The exponential law of endurance tests,” *Proc. Am. Soc. Test.*

Mater., vol. 10, no. 2, pp. 625–630.

[25] G. T. Mark and A. S. Gozdz, “Three dimensional printer for fiber reinforced composite filament fabrication,” U.S. Patent 20160361869A1, 2015.

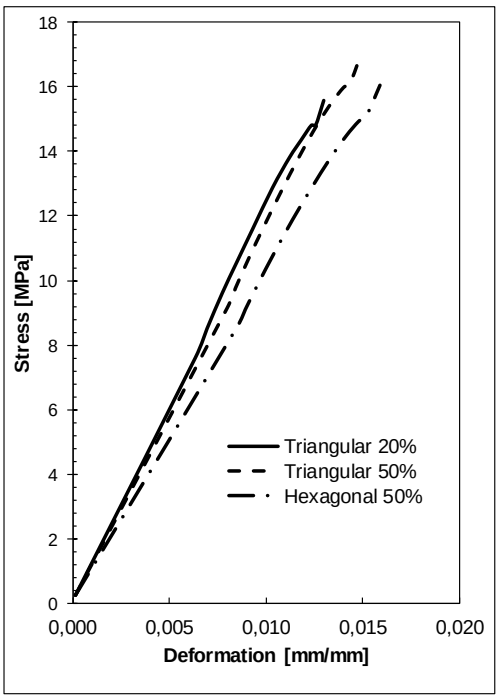

Figure 1. Uniaxial tensile test curves, pattern and fill percentage selections.

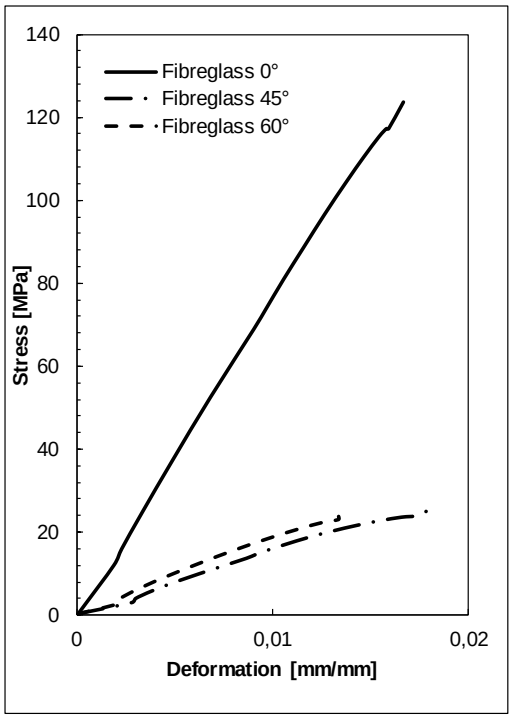

Figure 2. Uniaxial tensile test curves, nylon matrix with triangular filling pattern at 20%. Fibreglass as reinforcement material at 0°, 45° and 60° orientations.

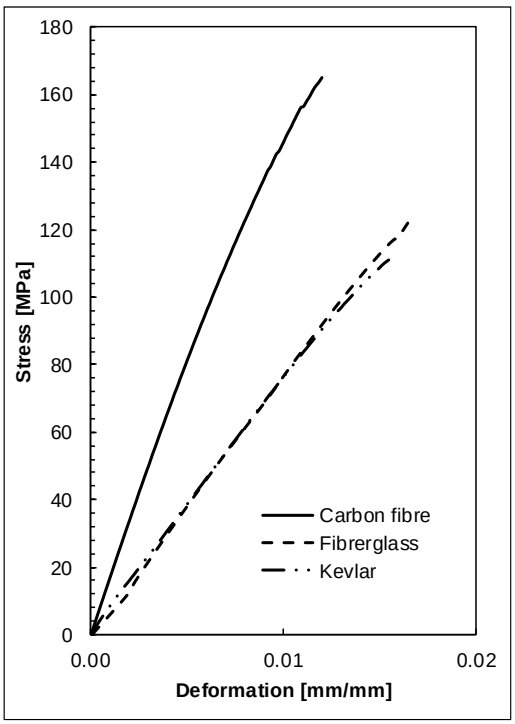

Figure 3. Uniaxial tensile test curves, nylon matrix with triangular filling pattern at 20%. Kevlar, carbon and glass fibres as reinforcement material at 0° orientations.

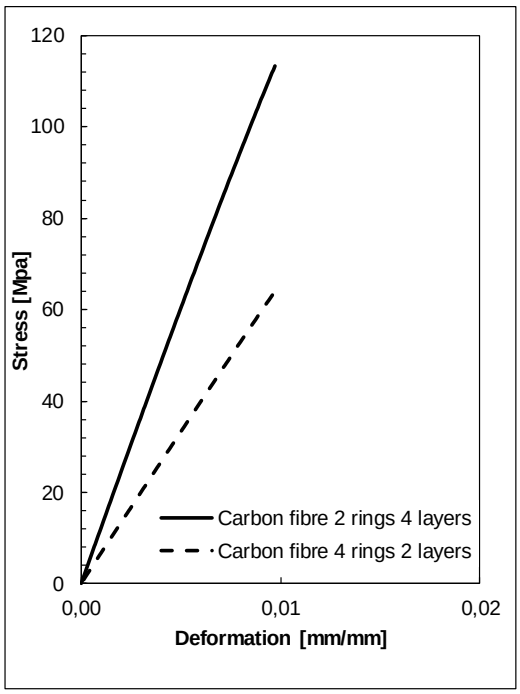

Figure 4. Uniaxial tensile test curves, nylon matrix with the triangular filling pattern, 20% of filling percentage, carbon fibre 2 rings 4 layers reinforcement and carbon fibre 4 rings 2 layers reinforcement.

Table 1. Printing parameters used for manufacturing tensile and fatigue test specimens.

Printing parameters	Nylon matrix	Isotropic	Concentric rings
Layer height (mm)	0,1	0,1	0,1
Filling percentage (%)	20, 50	20	20
Filling pattern	Triangular, Hexagonal	Triangular	Triangular
Filling layers	24	18	24
Walls	2	2	2
Top layers	4	4	4
Bottom layers	4	4	4
Fibre layer		6	4, 2
Fibre distribution		Isotropic	Concentric rings
Fibre angle		0°, 45°, 90°	
Concentric rings			2, 4
Total layers	32	32	32

Table 2. Variables of the experiment in the first stage, Matrix Fill (%) and Pattern Fill.

Filling percentage (%)	Filling pattern	Load levels (%)
20, 50	Triangular, Hexagonal	95, 90, 85 80

Table 3. Data obtained from the experiments related to the specimens with filling patterns triangular 20, 50%, and hexagonal 50%.

Samples	Stress (S) MPa.	Cycles (N_f)	Stress (S) MPa.	Cycles (N_f)	Stress (S) MPa.	Cycles (N_f)	Stress (S) MPa.	Cycles (N_f)
	Hexagonal filling pattern and 50% filling percentage							
1	15,2 (95% S_{UT})	165	14,4 (90% S_{UT})	269	13,6 (85% S_{UT})	267	12,8 (80% S_{UT})	459
2		136		250		267		295
3		196		245		271		393
4		128		230		245		360
5		176		253		258		420
Weibull mean probability		160		249		262		386
	Triangular filling pattern and 20% filling percentage							
1	14,8 (95% S_{UT})	222	14,0 (90% S_{UT})	370	13,2 (85% S_{UT})	397	12,5 (80% S_{UT})	597
2		249		344		205		725
3		250		351		463		316
4		210		325		185		427
5		230		312		364		528
Weibull mean probability		232		340		354		551
	Triangular filling pattern and 50% filling percentage							
1	16,2 (95% S_{UT})	219	15,4 (90% S_{UT})	328	14,5 (85% S_{UT})	363	13,7 (80% S_{UT})	538
2		223		229		382		359
3		196		268		426		343
4		186		298		354		440
5		230		253		402		335
Weibull mean probability		211		275		385		402

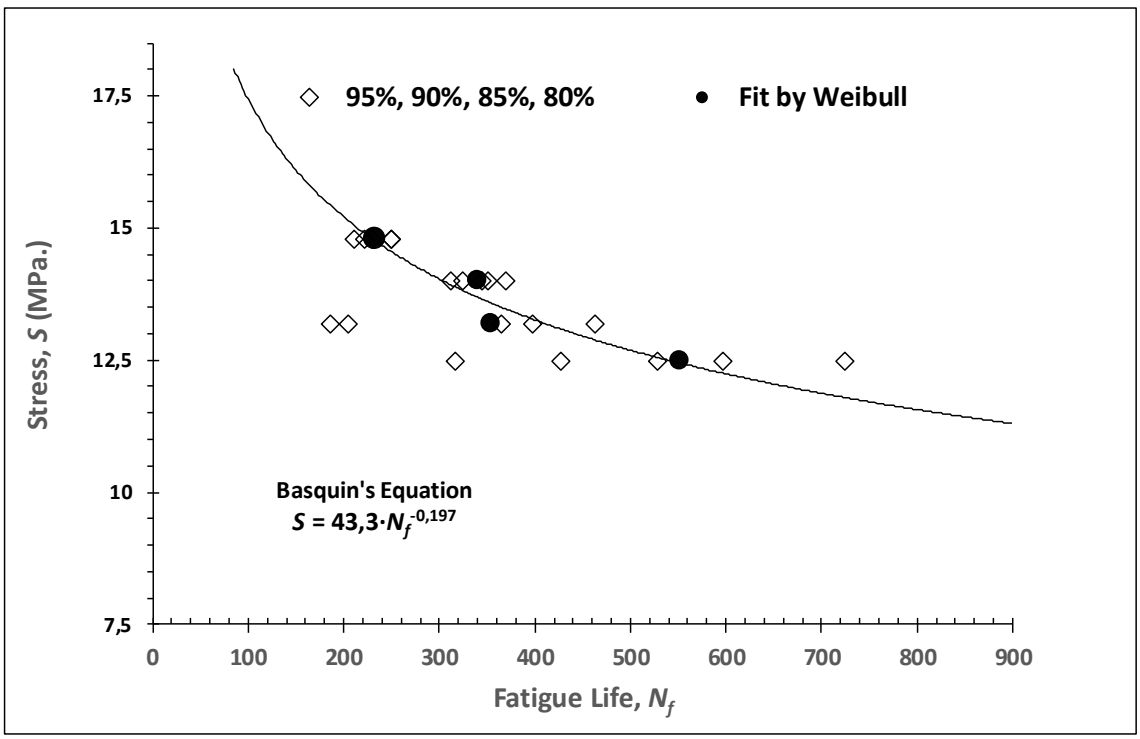

Figure 5. *S* vs N_f curves fitted to the Basquin´s model, for nylon matrix with triangular filling pattern and 20% of filling percentage.

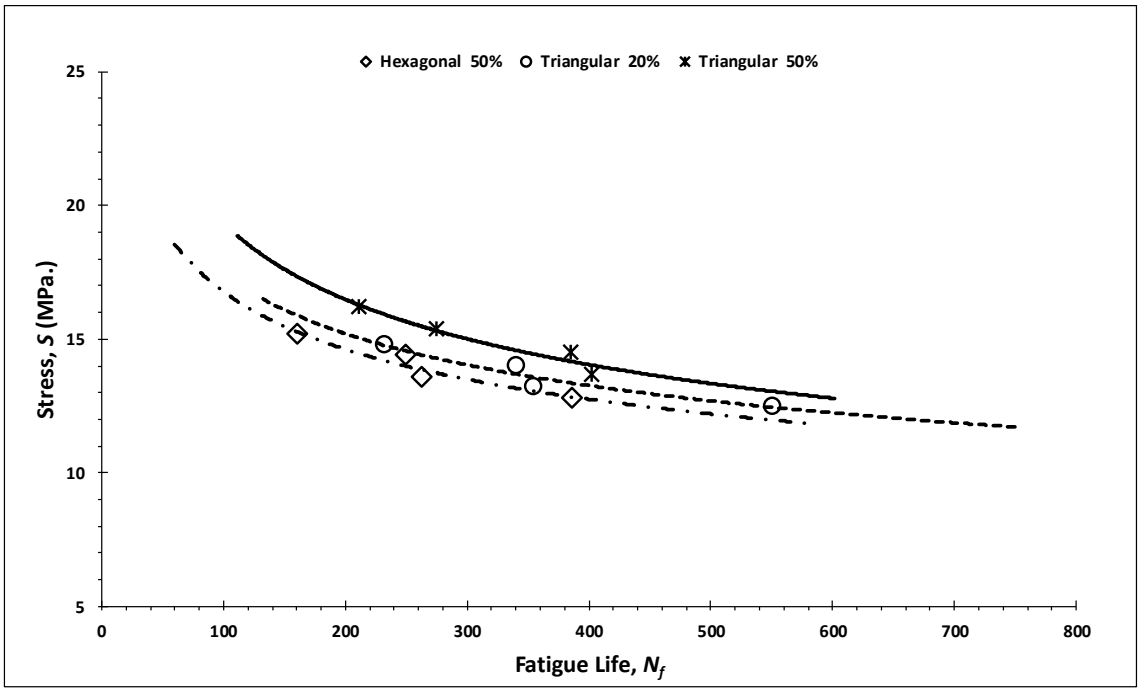

Figure 6. *S* vs N_f curves fitted to the Basquin´s model, filling pattern of triangular 20%, 50%, and hexagonal 50%.

Table 4. Values *A* and *b* of Basquin's relation, filling pattern of triangular 20, 50%, and hexagonal 50%.

Filling pattern	*A*	*b*	R^2
Triangular 50%	55,9	-0,231	0,93
Triangular 20%	43,3	-0,197	0,92
Hexagonal 50%	41,7	-0,198	0,93

Table 5. Variables of the experiment in the second stage for fibre orientation.

Filling percentage (%)	Filling pattern	Reinforcement material	Fibre orientation(°)	Load levels (%)
20	Triangular	Fibreglass	0, 45, 60	95, 90, 85 80

Table 6. Data obtained from the experiments related to the specimens with triangular filling pattern and 20% filling percentage, fibreglass as reinforcement material at 0, 45, and 60 degrees.

Samples	Stress (S) MPa.	Cycles (N_f)	Stress (S) MPa.	Cycles (N_f)	Stress (S) MPa.	Cycles (N_f)	Stress (S) MPa.	Cycles (N_f)
	Triangular filling pattern and 20% filling percentage, reinforced with fibreglass 0 degrees.							
1	117,4 (95% S_{UT})	31	111.2 (90% S_{UT})	176	105 (85% S_{UT})	317	98,8 (80% S_{UT})	510
2		42		170		234		503
3		88		114		259		503
4		28		182		348		550
5		93		104		246		527
Weibull mean probability		57		150		281		518
	Triangular filling pattern and 20% filling percentage, reinforced with fibreglass 45 degrees.							
1	24,6 (95% S_{UT})	127	23,3 (90% S_{UT})	123	22,0 (85% S_{UT})	223	20,1 (80% S_{UT})	311
2		46		184		270		181
3		52		105		302		416
4		84		166		214		280
5		101		167		254		308
Weibull mean probability		82		150		252		299
	Triangular filling pattern and 20% filling percentage, reinforced with fibreglass 60 degree.							
1	23,3 (95% S_{UT})	83	22,1 (90% S_{UT})	342	20,8 (85% S_{UT})	419	19,6 (80% S_{UT})	538
2		125		361		437		494
3		101		259		471		562
4		85		318		419		412
5		80		271		459		508
Weibull mean probability		94		311		441		504

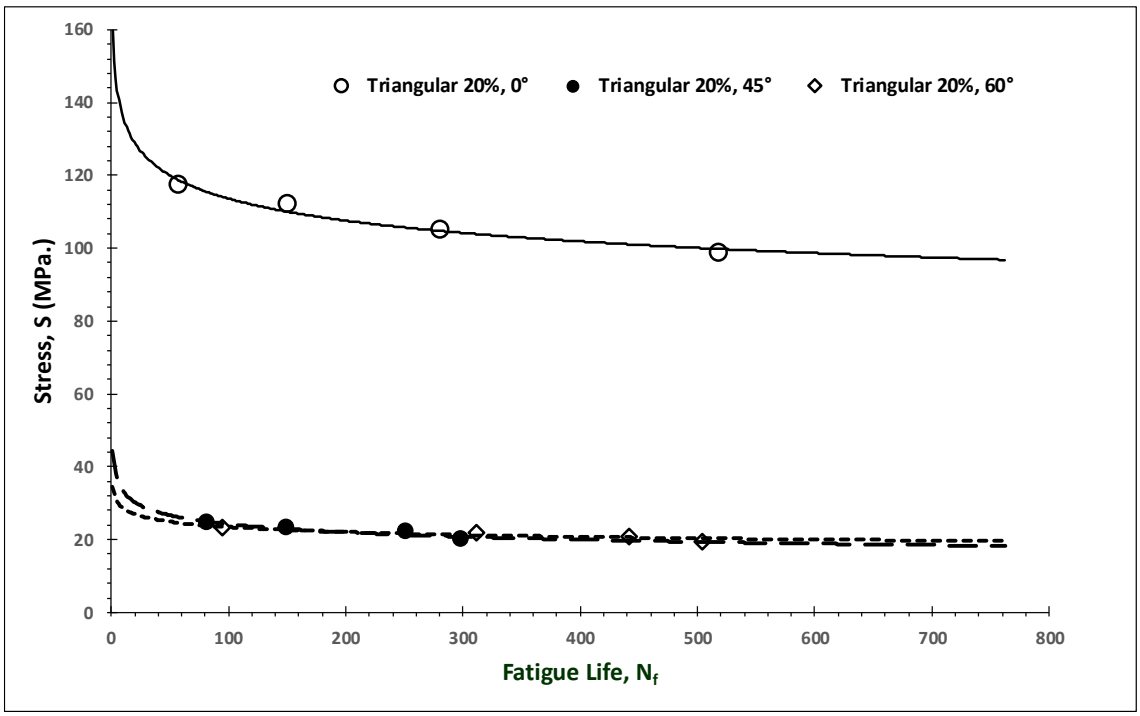

Figure 7. *S* vs N_f curves fitted to the Basquin´s model, nylon matrix with the triangular filling pattern, 20% of filling percentage, reinforced with fibreglass to 0, 45, 60 degrees.

Table 7. Values *A* and *b* of Basquin's parameters for a nylon matrix with triangular filling pattern, 20% of filling percentage, reinforced with fibreglass at 0, 45, and 60 degrees.

Material	*A*	*b*	R^2
Fibreglass, 0°	163	-0,079	0,99
Fibreglass, 45°	46	-0,139	0,88
Fibreglass, 60°	35	-0,088	0,81

Table 8. Variables of the experiment for fibre reinforcement material.

Filling percentage (%)	Fill pattern	Reinforcement material	Fibres orientation(°)	Load levels (%)
20	Triangular	Fibreglass, Kevlar, carbon	0	95, 90, 85 80

Table 9. Data obtained from the experiments related to the specimens with triangular filling pattern and 20% of filling percentage and fibreglass, Kevlar, and carbon fibre as reinforcement material at 0 degrees orientation.

Samples	Stress (S) MPa.	Cycles (N_f)	Stress (S) MPa.	Cycles (N_f)	Stress (S) MPa.	Cycles (N_f)	Stress (S) MPa.	Cycles (N_f)
	Carbon fibre							
1	157 (95% S_{UT})	1395	148,6 (90% S_{UT})	10393	140,4 (85% S_{UT})	41189	132,2 (80% S_{UT})	72023
2		202		14579		4936		75934
3		351		8145		28635		93629
4		1452		5987		32612		97117
5		1463		7605		38520		60996
Weibull mean probability		968		9352		10393		80075
	Kevlar fibre							
Samples	Stress (S) MPa.	Cycles (N_f)	Stress (S) MPa.	Cycles (N_f)	Stress (S) MPa.	Cycles (N_f)	Stress (S) MPa.	Cycles (N_f)
1	105,5 (95% S_{UT})	10	100 (90% S_{UT})	48	94,5 (85% S_{UT})	112	88,8 (80% S_{UT})	876
2		14		70		433		2532
3		2		68		322		1600
4		26		152		224		1075
5		29		52		114		1024
Weibull mean probability		16		78		242		1428
	Fibreglass							
Samples	Stress (S) MPa.	Cycles (N_f)	Stress (S) MPa.	Cycles (N_f)	Stress (S) MPa.	Cycles (N_f)	Stress (S) MPa.	Cycles (N_f)
1	117,4 (95% S_{UT})	31	111.2 (90% S_{UT})	176	105 (85% S_{UT})	317	98,8 (80% S_{UT})	510
2		42		170		234		503
3		88		114		259		503
4		28		182		348		550
5		93		104		246		527
Weibull mean probability		57		150		281		518

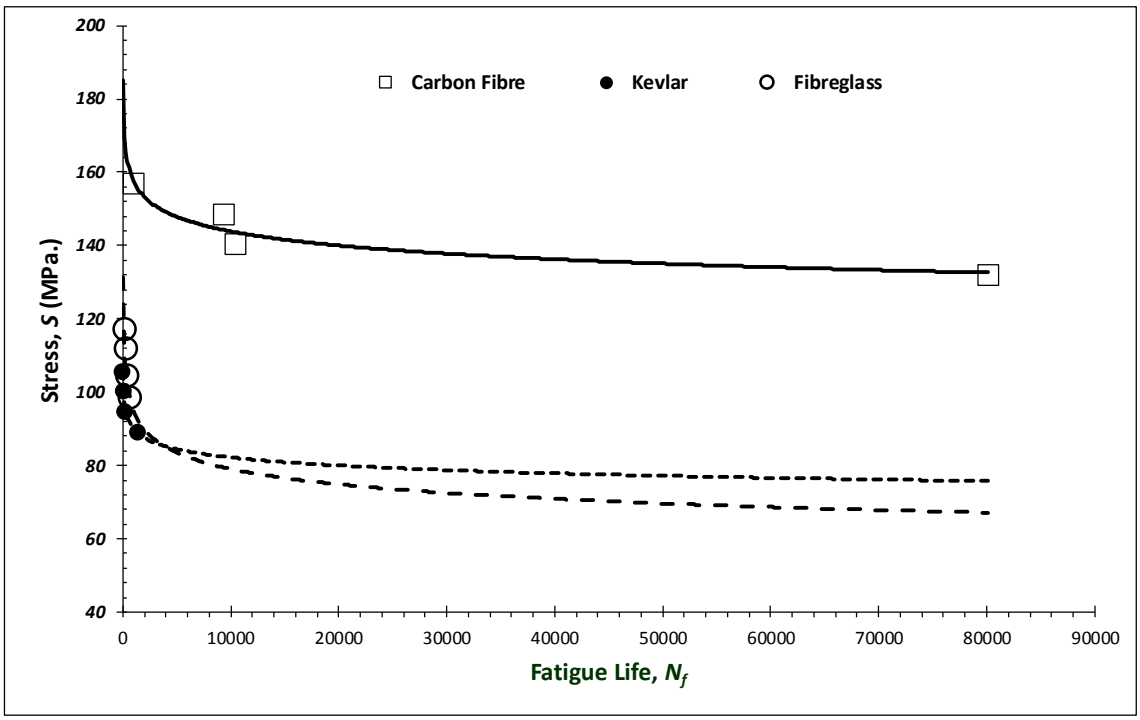

Figure 8. *S* vs N_f curves fitted to the Basquin´s model, nylon matrix with the triangular filling pattern, 20% of filling percentage, reinforced with fibreglass, Kevlar and carbon fibre at 0 degrees orientation.

Table 10. The values *A* and *b* of Basquin's parameters, nylon matrix with the triangular filling pattern, 20% of filling percentage, reinforced with fibreglass, Kevlar and carbon fibre at 0 degrees orientation.

Material	*A*	*b*	R^2
Carbon	206	-0.039	0,91
Kevlar	118	-0,039	0,96
Fibreglass	163	-0,079	0,99

Table 11. Variables of the experiment for ring-type reinforcements.

Filling percentage (%)	Filling pattern	Reinforcement material	Ring-type, layers reinforcements	Load Levels (%)
20	Triangular	Carbon fibre	2, 4	95, 90, 85 80

Table 12. Results for the specimens with triangular filling pattern and 20% of filling percentage, with different Carbon fibre rings and layers.

Samples	Stress (S) MPa.	Cycles (N_f)	Stress (S) MPa.	Cycles (N_f)	Stress (S) MPa.	Cycles (N_f)	Stress (S) MPa.	Cycles (N_f)
	Carbon fibre, 2 rings, 4 layers							
1	107,7 (95% S_{UT})	425	102,2 (90% S_{UT})	38076	96,4 (85% S_{UT})	2052	90,9 (80% S_{UT})	40675
2		566		4		81799		32897
3		294		72050		5614		47635
4		191		15789		43925		351667
5		347		65245		3439		44552
Weibull mean probability		365		57770		27223		40233
	Carbon fibre, 4 rings, 2 layers							
1	61,5 (95% S_{UT})	211	58,4 (90% S_{UT})	5019	55 (85% S_{UT})	9071	51,9 (80% S_{UT})	35321
2		102		16		7675		31857
3		115		95		86		2735
4		3		1		3174		33278
5		78		11		246		38240
Weibull mean probability		101		941		4251		27510

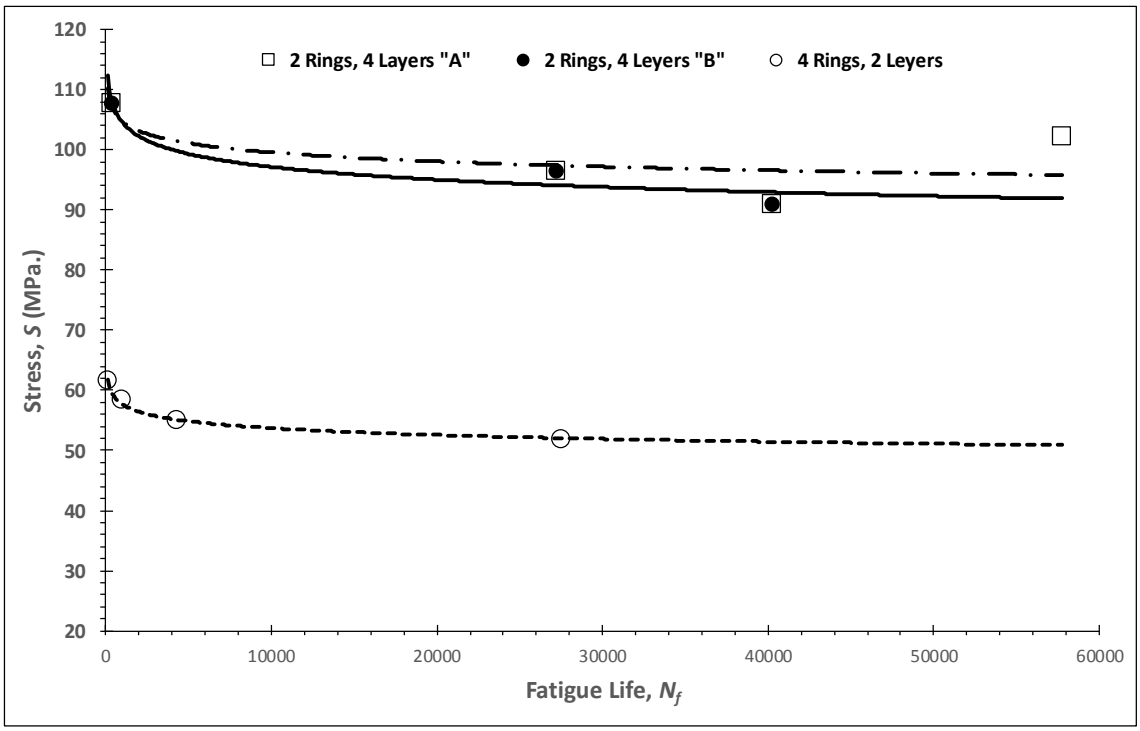

Figure 9. *S* vs N_f curves fitted to the Basquin´s model, nylon matrix with the triangular filling pattern, 20% of filling percentage, and varying carbon fibre rings and layers.

Table 13. The values *A* and *b* of Basquin's parameters nylon matrix with the triangular filling pattern, 20% of filling percentage, and varying carbon fibre rings and layers.

Material	*A*	*b*	R^2
2 Rings, 4 Layers, "A"	122	-0,022	0,5
2 Rings, 4 Layers, "B"	130	-0.032	0,92
4 Rings, 2 Layers	71,3	-0,031	0,98

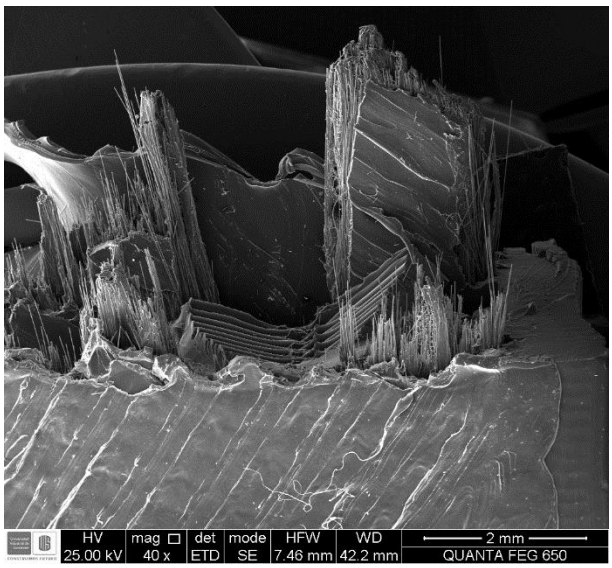

Figure 1. SEM image shows the fracture of the specimen with the triangular filling pattern, 20% of filling percentage, and carbon fibre as reinforcement material at 0° orientation and 80% of Sut.

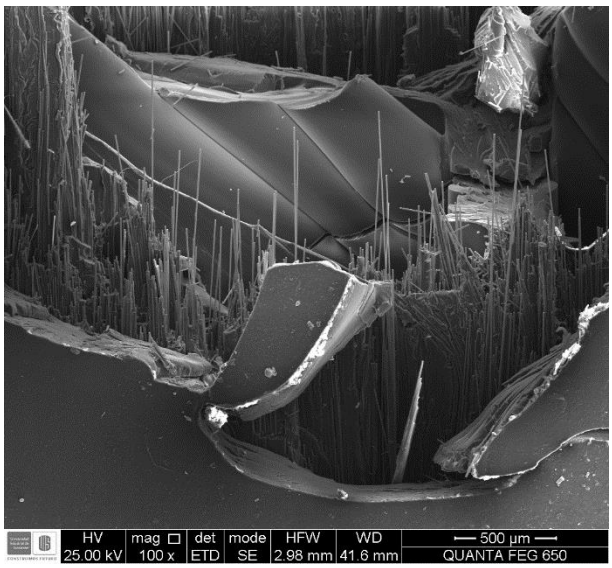

Figure 2. SEM image shows the fracture of the specimen with the triangular filling pattern, 20% of filling percentage, and carbon fibre as reinforcement material at 0° orientation and 95% of Sut.

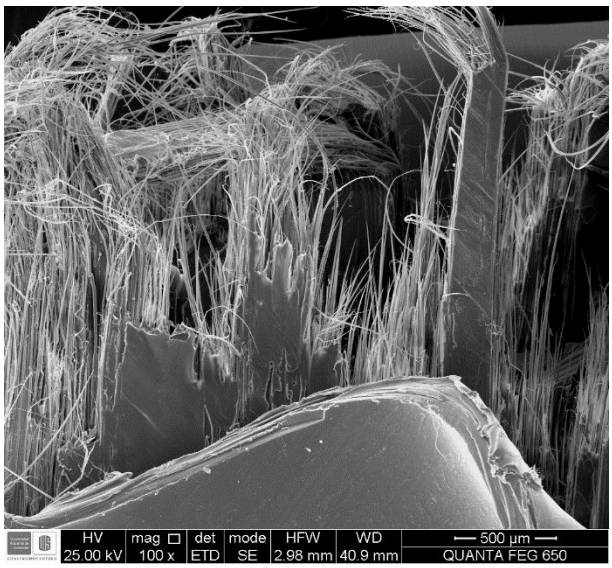

Figure 3. SEM image shows the fracture of the specimen with the triangular filling pattern, 20% of filling percentage, and Kevlar fibre as reinforcement material at 0° orientation and 80% of Sut.

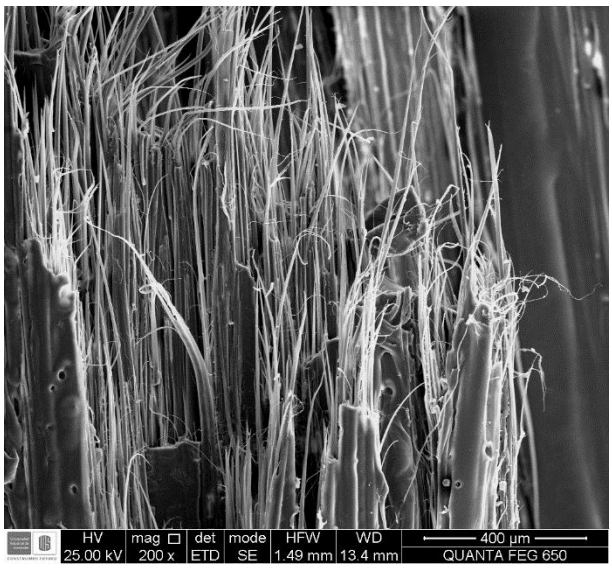

Figure 4. SEM image shows the fracture of the specimen with the triangular filling pattern, 20% of filling percentage and Kevlar fibre as reinforcement material at 0° orientation and 95% of Sut.